

RESEARCH LETTER

10.1002/2014GL060473

Key Points:

- Spin crossover in liquid Fe_2SiO_4 is studied at high pressure and temperature
- High-spin to low-spin transition is smooth over a broad pressure interval
- Silicate melts may be buoyantly stable at the base of Earth's mantle

Supporting Information:

- Readme
- Figures S1–S4 and Tables S1–S4

Correspondence to:

D. Muñoz Ramo,
dm586@cam.ac.uk

Citation:

Muñoz Ramo, D., and L. Stixrude (2014), Spin crossover in Fe_2SiO_4 liquid at high pressure, *Geophys. Res. Lett.*, 41, 4512–4518, doi:10.1002/2014GL060473.

Received 8 MAY 2014

Accepted 18 JUN 2014

Accepted article online 24 JUN 2014

Published online 8 JUL 2014

Spin crossover in Fe_2SiO_4 liquid at high pressureDavid Muñoz Ramo^{1,2} and Lars Stixrude¹

¹Department of Earth Sciences, University College London, London, UK, ²Department of Materials Science and Metallurgy, University of Cambridge, Cambridge, UK

Abstract We combine spin-polarized density functional theory with first principle molecular dynamics (FPMD) to study the spin crossover in liquid Fe_2SiO_4 , up to 300 GPa and 6000 K. In contrast to the much sharper transition seen in crystals, we find that the high- to low-spin transition occurs over a very broad pressure interval (>200 GPa) due to structural disorder in the liquid. We find excellent agreement with the experimental Hugoniot. We combine our results with previous FPMD calculations to derive the partial molar volumes of the oxide components MgO, FeO, and SiO_2 . We find that eutectic melts in the MgO-FeO- SiO_2 system are denser than coexisting solids in the bottom 600 km of Earth's mantle.

1. Introduction

Knowledge of the physical properties of silicate melts is crucial for understanding the chemical and thermal evolution of the Earth. Seismological studies suggest the existence of melts in the present-day Earth up to pressure-temperature conditions of the core-mantle boundary (136 GPa, 4000 K) [Williams and Garnero, 1996]. Melts at high pressure may have been even more important in the early Earth, when most or all of the mantle may have been molten [Labrosse et al., 2007; Stixrude et al., 2009].

A key question relates to the buoyancy of melts at great depth: are they less dense than coexisting solids, in which case they rise to the surface like near-surface melts or are they more dense in which case they remain trapped at depth? The role of iron is central: iron is the heaviest of the terrestrially abundant cations, and it is known to partition into the liquid phase on partial melting [Andrault et al., 2012].

Iron behaves differently from other major cations: iron-bearing silicates are expected to be paramagnetic in the mantle. The temperature in Earth's mantle far exceeds magnetic ordering temperatures (65 K for fayalite), so magnetic moments are disordered. Nevertheless, local moments survive because mantle temperatures are much less than typical Fermi temperatures (70,000 K for fayalite). High pressure can alter the magnitude of the local moments by causing a high-spin to low-spin transition. This magnetic collapse is generic to Fe oxide and silicate systems because it is driven by d-band broadening on compression [Cohen et al., 1997]. The transition is important geophysically because it influences the density and the partitioning of iron among coexisting phases [Badro et al., 2003; Tsuchiya et al., 2006]. Experiments have so far been unable to measure the spin state in silicate liquids at elevated pressure.

First principles theory has not yet been applied to the study of iron-bearing silicate liquids, and experimental data at lower mantle conditions are limited [Thomas et al., 2012]. Liquid Fe_2SiO_4 has been studied by classical molecular dynamics [Guillot and Sator, 2007], but this method cannot address the relevant physics, including the spin transition, and is further limited by the uncertainty in the choice of the interatomic potential. Here we use first principle molecular dynamics (FPMD) based on density functional theory, in which the relevant physics are readily captured.

2. Computational Method

All of our calculations are based on the Perdew-Burke-Ernzerhof (PBE) form of the generalized gradient approximation [Perdew et al., 1996], with spin polarization to correctly capture the physics of local magnetic moments. In order to account for the strong coulombic interactions between *d* electrons, we use the rotationally invariant Hubbard *U* formalism (PBE+*U*) [Anisimov et al., 1997], which applies an energetic penalty *U* to the double occupation of the *d* orbitals. We adopt the value $U = 4.75$ eV computed self-consistently via density functional perturbation theory in fayalite [Cococcioni and de Gironcoli, 2005]. For comparison, we also perform a series of simulations with $U = 0$ (PBE) in order to evaluate the influence of the value of *U* on our results.

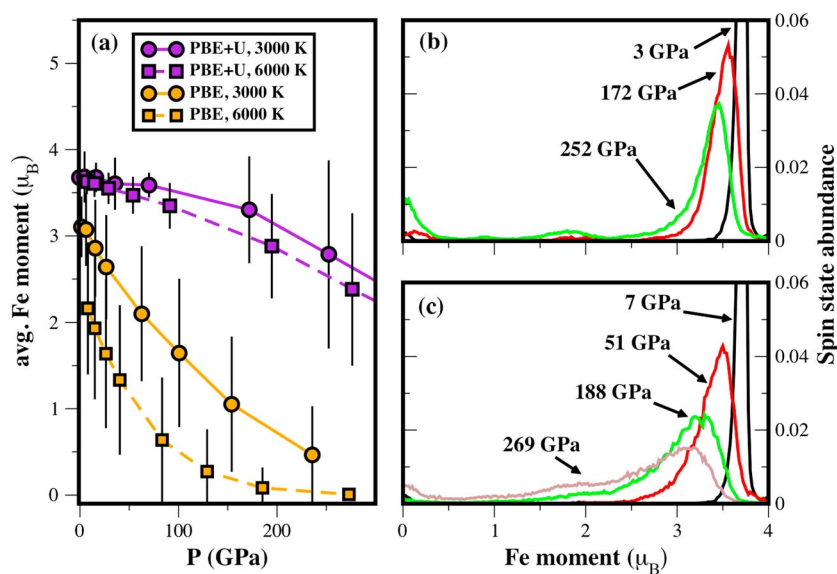


Figure 1. (a) Mean absolute local moment for PBE+U (purple) and PBE (orange): symbols are the FPMD results, and lines are a guide to the eye. Vertical bars at each point indicate the standard deviation of the spin state of the Fe ions. Histograms of the absolute local magnetic moment in PBE+U calculations at (b) 3000 K and (c) 6000 K.

Other technical details follow our previous FPMD simulations of silicate liquids [Stixrude and Karki, 2005; de Koker et al., 2013]. We used the projector-augmented wave implementation [Kresse and Joubert, 1999] and an energy cutoff of 500 eV for the plane wave basis set. For Fe, Si, and O the potentials treat, respectively, 14, 4, and 6 electrons as valence; the core radii are 1.16 Å, 0.79 Å, and 0.80 Å, respectively, which ensures that there was no significant core overlap over the pressure range considered. Calculations were performed at the gamma point in the canonical ensemble using the Vienna Ab-initio Simulation Package [Kresse and Furthmüller, 1996], with a time step of 1 fs, for at least 3000 time steps. The initial condition is a $2 \times 2 \times 1$ supercell of fayalite with 112 atoms, uniformly strained to a cubic shape. For each volume, the cell was melted at 6000 K and then cooled to 4000 K and 3000 K. We explore the range of volumes $V/V_x = 1.2$ –0.45 where for convenience we scale the volume to $V_x = 55.34 \text{ cm}^3/\text{mol}$, the volume of the Fe_2SiO_4 liquid at the ambient melting point [Shiraishi et al., 1978]. Some runs were also performed at 2000 K in the range $V/V_x = 1.2$ –0.9 to better constrain low-pressure properties. We assume thermal equilibrium between ions and electrons via the Mermin functional [Mermin, 1965; Wentzcovitch et al., 1992]. We confirmed that the choice of initial magnetic structure did not influence our results (see supporting information).

In order to analyze our results, we fit FPMD values of internal energy and pressure to the fundamental thermodynamic relation of de Koker and Stixrude [2009]. This procedure allows us to derive self-consistently all thermodynamic properties, including second-order properties guaranteed to satisfy the Maxwell relations. More details can be found in the supporting information.

The theoretical Hugoniot is computed as the set of state points that satisfy the Rankine-Hugoniot relation

$$(E_H - E_R) = -\frac{1}{2}(P_H + P_R)(V_R - V_H). \quad (1)$$

Following previous studies [de Koker and Stixrude, 2009], we find the value of the temperature (T_H) at given volume (V_H) that yields values of the internal energy (E_H) and pressure (P_H) such that the relation is satisfied. Subscript R refers to the unshocked reference state. We compute theoretical Hugoniots for two ambient pressure ($P_R = 0$) reference states: liquid at $T_R = 1573 \text{ K}$ and $V_R/V_x = 1$ and crystalline fayalite at $T_R = 300 \text{ K}$ and $V_R/V_x = 0.8365$. We calculate E_R from the fundamental relation described above for the liquid reference state and from a spin-polarized PBE+U static calculation on the antiferromagnetic ground state for the solid reference state.

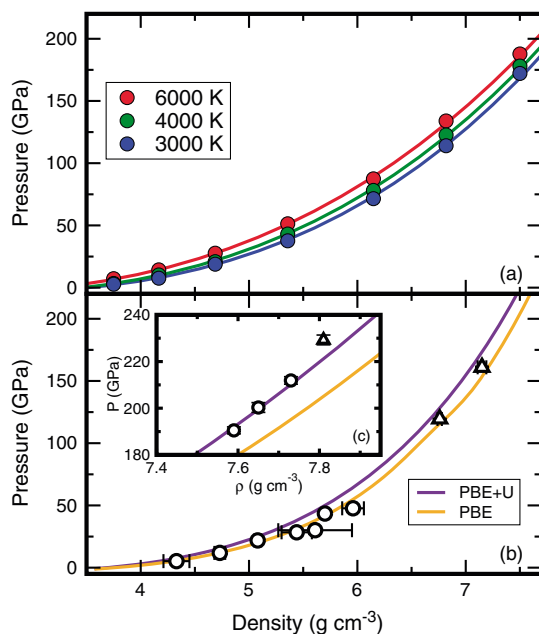


Figure 2. (a) Our PBE+U results (symbols) and the equation of state fit (lines). Hugoniot of (b) the preheated liquid ($T_R = 1573$ K) and (c) crystalline forsterite ($T_R = 300$ K) as computed from PBE+U (purple line) and PBE (orange line) and experimentally measured (symbols) [Chen *et al.*, 2002; Thomas *et al.*, 2012].

The gradual magnetic collapse in the liquid is very different from the behavior in solid oxides and silicates. In solids, the magnetic collapse is completed within a pressure interval <20 GPa at 300 K and, even at 2200 K, takes place over an interval less than 40 GPa [Mao *et al.*, 2011; Nomura *et al.*, 2011]. We attribute the different behavior of the liquid to the much greater variety of Fe coordination environments as compared with crystals or glass. Analysis of the radial distribution function from our simulations shows a wide range of Fe-O bond lengths in the liquid with standard deviation $\sigma = 0.21$ Å (see supporting information). This is in contrast to the much narrower range of divalent cation oxygen bond lengths in silicate glasses, $\sigma = 0.108$ Å [Waseda and Toguri, 1977], similar to the value for crystalline fayalite ($\sigma = 0.079$ Å).

We find excellent agreement with shock wave measurements (Figure 2). PBE+U yields slightly smaller densities along the Hugoniot as compared with PBE. This difference is consistent with the greater mean

3. Results

Our simulations show a very broad high- to low-spin transition in the liquid taking place over a pressure interval >200 GPa (Figure 1). In PBE+U calculations, the transition is not complete even up to the highest pressures of our study (300 GPa), whereas in PBE calculations, the liquid is almost entirely low spin by 250 GPa. The tendency for the local moment magnitude to decrease with compression is already apparent at ambient pressure. The larger local moments in PBE+U as compared with PBE are consistent with expectations: the stronger local correlation produced by the finite value of U favors the high-spin state [Stackhouse *et al.*, 2010].

The transition takes place in the liquid by altering the relative proportions of high- and low-spin cations (Figure 1). Histograms of local moment magnitudes are bimodal with most Fe cations either high or low spin, and a small proportion in an intermediate-spin state ($\approx 2\mu_B$). For example, the system is essentially 100% high spin at 3 GPa and 71% high spin, 22% low spin, and 7% intermediate spin at 252 GPa.

local moment magnitude in PBE+U: larger local moments lead to lower density. By comparison, the Hugoniot computed from classical potentials is much too stiff as compared with experimental data: the pressure is overestimated by 40% [Guillot and Sator, 2007].

The importance of +U is shown by comparison to the experimental heat capacity (Table 1): the PBE+U value agrees well with experiment, while the PBE value is much too high. We have traced the origin of this difference to the electronic structure: while PBE+U shows a pseudogap, PBE has a large density of states at the Fermi level (Figure 3). This means that PBE has a large electronic contribution to the heat capacity that is not

Table 1. Properties of Liquid Fe_2SiO_4 Calculated Using Fundamental Thermodynamic Relation at Ambient Pressure and $T_0 = 1573$ K, Compared With Experiment and Classical MD Simulations [Guillot and Sator, 2007]

	PBE	PBE+U	Classical MD	Experiment
ρ_0 (g/cm ³)	3.811	3.687	3.75	3.750 ^a
K_S (GPa)	23.9	25.3	22.0	25.9 ^b , 21.4 ^c
C_p (NK _B)	4.932	3.906	4.013	4.133 ^d
$10^5 \cdot \alpha$ (K ⁻¹)	5.38	5.94	12.8	5.7 ^e , 7.1 ^a
γ_0	0.24	0.37	0.521	0.33 ^{a,b,d,e}

^aShiraishi *et al.* [1978].

^bChen *et al.* [2002].

^cRivers and Carmichael [1987].

^dOrr [1953].

^eCourtial *et al.* [1997].

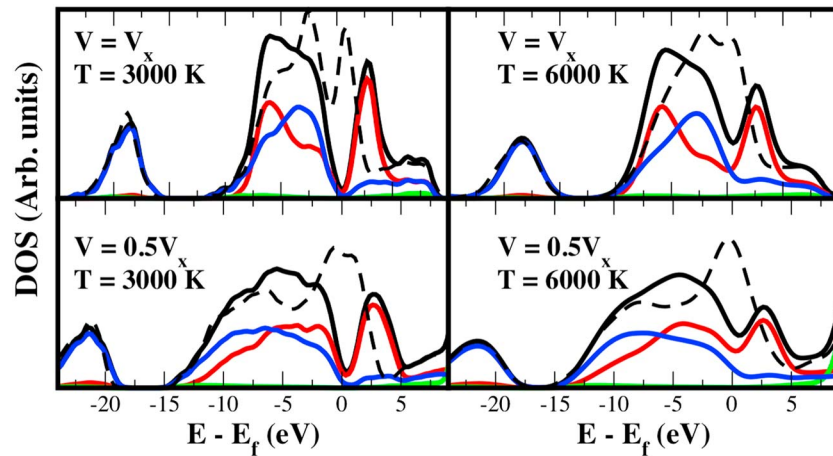


Figure 3. Average electronic density of states (DOS) of liquid Fe_2SiO_4 using the PBE+U functional: total DOS (black), oxygen contribution (blue), iron contribution (red), and silicon contribution (green). Dashed black line is the total DOS with PBE.

observed experimentally: the experimental value is very similar to that of Mg-silicate liquids. The pseudogap that we find in PBE+U is also consistent with experimental measurements of the current efficiency, which show that the dominant charge carriers are ions rather than electrons and that the liquid is at best a semiconductor [Simnad and Derge, 1953]. The influence of U in our calculations is similar to that seen in crystalline systems: Fe oxides and silicates are observed experimentally to be insulators at low pressure and incorrectly predicted to be metals by PBE, whereas PBE+U produces a gap comparable in magnitude to that observed experimentally [Cococcioni and de Gironcoli, 2005; Stackhouse et al., 2010].

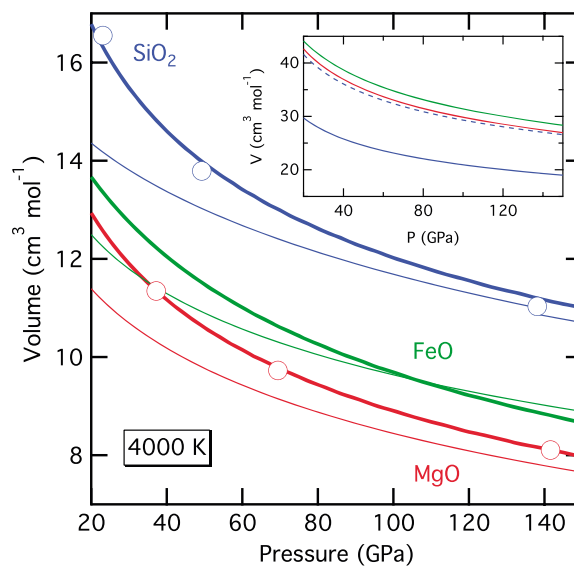


Figure 4. Partial molar volume of the oxides in the liquid state (thick solid lines) as derived from FPMD results on Fe_2SiO_4 (present work), Mg_2SiO_4 , and MgSiO_3 [de Koker et al., 2013] compositions. Partial molar volumes are compared with independent FPMD simulations on the pure end-member oxides MgO and SiO_2 [de Koker et al., 2013] (symbols). Thin lines show the equation of state of the crystalline oxides as computed with HeFESTo [Stixrude and Lithgow-Bertelloni, 2011]. The inset shows the equations of state of Fe_2SiO_4 (green), Mg_2SiO_4 (red), and MgSiO_3 (blue) liquids. The blue-dashed line shows the volume of MgSiO_3 multiplied by 7/5 to permit direct comparison, on a per atom basis, with the orthosilicate compositions.

As pressure increases, the electronic structure of fayalite liquid computed with PBE+U changes and the gap closes (Figure 3). At conditions corresponding to those at the base of Earth's mantle, the liquid shows a large density of states at the Fermi level. The closure of the pseudogap at high pressure suggests that fayalite liquid may be electrically conductive, i.e., metallic, in the deep mantle. The gap closes at much lower pressure than in iron-free silicate liquids [Hicks et al., 2006; Spaulding et al., 2012; McWilliams et al., 2012], and amorphous Fe_2SiO_4 formed by compression of fayalite at room temperature [Williams et al., 1990]. The role of iron must be taken into account in assessing the possible existence and geophysical significance of electrically conducting silicate liquids in planetary interiors.

We gain additional insight into the equation of state of silicate liquids by comparing with previous results on Mg_2SiO_4 and MgSiO_3 compositions [de Koker et al., 2013] (Figure 4). As expected, the volume of Fe_2SiO_4 composition is slightly greater than that of Mg_2SiO_4 , reflecting the larger ionic radius of Fe as

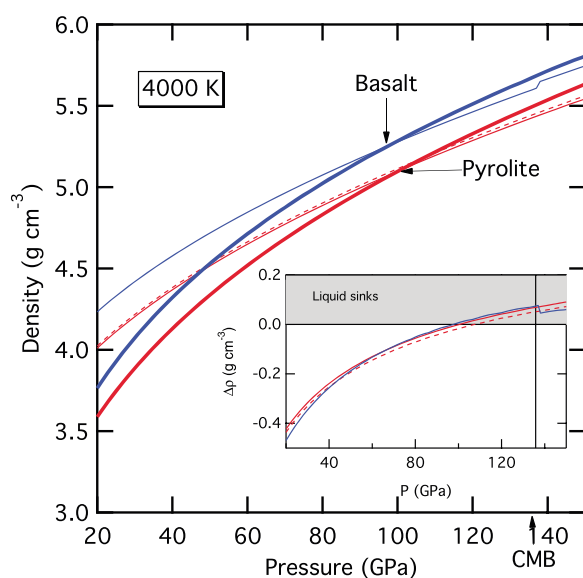


Figure 5. Density of crystalline assemblages of pyrolite (thin red) and basalt (thin blue) compositions compared with the density of partial melts in equilibrium with these compositions (bold lines). The dashed line estimates the influence of the high- to low-spin transition in ferropericlase by assuming that the low-spin phase is 2% denser [Mao *et al.*, 2011]. The inset shows the density difference between pyrolite and its partial melt (red) and basalt and its partial melt (blue). Solid assemblage mass fractions at the core-mantle boundary as computed with HeFESTo are 0.82, 0.46 (perovskite), 0.18, 0.06 (ferropericlase), and 0, 0.48 (stishovite) for pyrolite and basalt, respectively.

Earth (Figure 5). We compute the density of coexisting partial melts and crystalline assemblages in the MgO-FeO-SiO₂ system for two scenarios: partial melting of pyrolite and basalt, such as might occur in the lower thermal boundary layer at the base of the mantle. We approximate pyrolite and basalt as the eutectic compositions on the MgO-SiO₂ join [de Koker *et al.*, 2013], $Z = \text{SiO}_2 / (\text{SiO}_2 + \text{MgO} + \text{FeO}) = 0.405$ and $Z = 0.70$ respectively, and assume $X_{\text{Fe}} = \text{Fe} / (\text{Fe} + \text{Mg}) = 0.1$ and $X_{\text{Fe}} = 0.3$, for pyrolite and basalt respectively [Workman and Hart, 2005]. We assume Fe partitioning according to the Mg-Fe partition coefficient between Mg-rich silicate perovskite and liquid $K = 0.4$, consistent with experimental studies [Andrault *et al.*, 2012], yielding $X_{\text{Fe}} = 0.22$ and $X_{\text{Fe}} = 0.54$ for the two partial melts, respectively, in the limit of infinitesimal amounts of partial melt. Solid phase proportions, compositions, and physical properties are computed with HeFESTo [Stixrude and Lithgow-Bertelloni, 2011]. We find that partial melts of both compositions are denser than the coexisting solids at pressures exceeding 100 GPa, i.e., in the bottommost 600 km of the mantle.

4. Discussion and Conclusions

The gradual high- to low-spin transition that we find calls into question experimental evidence for sudden changes in the chemistry of silicate melts near 75 GPa [Nomura *et al.*, 2011]. For this behavior to be caused by magnetic collapse in the liquid, as inferred in the experimental study, the transition would have to occur over a very narrow pressure interval (<3 GPa) in contrast to the wide pressure interval that we find (>200 GPa). Magnetic collapse found in a glass compressed at 300 K [Nomura *et al.*, 2011] is not a good analog for the behavior of silicate liquids: the transition occurs over a much narrower pressure interval (<20 GPa) in the glass, which we attribute to the much greater degree of structural order in the glass as compared with the liquid. Based on the broad high- to low-spin transition that we find, we expect iron partitioning into the melt to increase slightly and gradually with increasing pressure, a conclusion supported by a recent experimental study [Andrault *et al.*, 2012].

For silicate melts to persist in the deep mantle they must be buoyantly stable, i.e., denser than surrounding crystalline material. Our results show that the influence of FeO on the density of silicate liquids is greater

compared with Mg. The volume difference diminishes slightly with increasing pressure reflecting the gradual magnetic collapse in Fe₂SiO₄. The volume per atom of MgSiO₃ is smaller than that of Mg₂SiO₄, consistent with the increase in density with increasing silica content across the MgO-SiO₂ join found in our previous work [de Koker *et al.*, 2013].

We apply a linear transformation to obtain the partial molar volumes of MgO, FeO, and SiO₂ components (Figure 4). We assume that the volume can be represented as a linear combination of partial molar oxide components since previous simulations have shown that the non-ideal volume of mixing on the MgO-SiO₂ join is only a few percent at lower mantle conditions [de Koker *et al.*, 2013]. The liquid components are all more compressible than their crystalline counterparts. In the case of FeO, the liquid component becomes denser than the high-spin crystalline component, reflecting the gradual magnetic collapse in the liquid.

We use these results to evaluate the buoyancy of partial melts in the deep

than we had estimated previously. Instead of the liquid-crystal density crossover occurring just above the core-mantle boundary [Stixrude *et al.*, 2009], we now find it to occur 600 km above the core-mantle boundary. The difference reflects the importance of the high- to low-spin transition in the liquid.

The presence of small amounts of dense partial melt provides a possible explanation of seismic anomalies in the lower mantle. According to our results, if partial melt exists it is slightly denser than surrounding mantle in the bottom 600 km of the mantle. While the position of the solidus with respect to lower mantle temperature remains a key uncertainty, recent measurements suggest that small amounts of partial melt may exist over a wide range of depth in the lower mantle [Nomura *et al.*, 2014]. Depending on the amount and geometry of partial melt, the melt may drain to the core-mantle boundary, producing melt-enriched regions that can explain ultralow velocity zones [Williams and Garnero, 1996; Stixrude *et al.*, 2009]. Alternatively, because the density contrast driving melt-crystal segregation is small, the partial melt may remain where it is formed. Widespread, laterally varying amounts of very low degree partial melts provide a natural explanation for the anomalously low shear wave velocity of the African and Pacific anomalies [Garnero *et al.*, 2007], and anomalously large lateral variations of shear as compared with compressional velocity [Robertson and Woodhouse, 1996; Duffy and Ahrens, 1992].

Acknowledgments

This research was funded by the UK National Environmental Research Council (Grant No. NE/F017871/1) and the European Research Council via the advanced grant MoltenEarth (Grant No. 291432). Calculations were performed on Legion, the University College London Research Computing facility, and HECToR, the UK national high-performance computing service.

The Editor thanks two anonymous reviewers for their assistance in evaluating this paper.

References

- Andraut, D., S. Petitgirard, G. Lo Nigro, J. Devidal, G. Veronesi, G. Garbarino, and M. Mezouar (2012), Solid-liquid iron partitioning in Earth's deep mantle, *Nature*, *487*, 354–357.
- Anisimov, V. I., F. Aryasetiawan, and A. I. Lichtenstein (1997), First-principles calculations of the electronic structure and spectra of strongly correlated systems: The LDA+U method, *J. Phys. Condens. Matter*, *9*, 767–808.
- Badro, J., G. Fiquet, F. Guyot, J.-P. Rueff, V. V. Struzhkin, V. György, and G. Monaco (2003), Iron partitioning in Earth's mantle: Toward a deep lower mantle discontinuity, *Science*, *300*, 789–791.
- Chen, G. Q., T. J. Ahrens, and E. M. Stolper (2002), Shock-wave equation of state of molten and solid fayalite, *Phys. Earth Planet. Inter.*, *134*, 35–52.
- Cococcioni, M., and S. de Gironcoli (2005), Linear response approach to the calculation of the effective interaction parameters in the LDA+U method, *Phys. Rev. B*, *71*, 035105.
- Cohen, R. E., I. I. Mazin, and D. G. Isaak (1997), Magnetic collapse in transition metal oxides at high pressure: Implications for the Earth, *Science*, *275*, 654–657.
- Courtial, P., E. Ohtani, and D. B. Dingwell (1997), High-temperature densities of some mantle melts, *Geochim. Cosmochim. Acta*, *61*, 3111–3119.
- de Koker, N. P., and L. Stixrude (2009), Self-consistent thermodynamic description of silicate liquids, with application to shock melting of MgO periclase and MgSiO₃ perovskite, *Geophys. J. Int.*, *178*, 162–179.
- de Koker, N., B. B. Karki, and L. Stixrude (2013), Thermodynamics of the MgO-SiO₂ liquid system in Earth's lowermost mantle from first principles, *Earth Planet. Sci. Lett.*, *361*, 58–63.
- Duffy, T. S., and S. K. Ahrens (1992), Lateral variation in lower mantle seismic velocities, in *High Pressure Research: Application to Earth and Planetary Sciences*, edited by Y. Syono and M. H. Manghnani, pp. 197–206, Terra Scientific, Tokyo.
- Garnero, E. J., T. Lay, and A. K. McNamara (2007), Implications of lower-mantle structural heterogeneity for the existence and nature of whole-mantle plumes, in *Plates, Plumes, and Planetary Processes*, edited by G. R. Fougere and D. M. Jurdy, pp. 79–109, Geol. Soc. Am., Boulder, Colo.
- Guillot, B., and N. Sator (2007), A computer simulation study of natural silicate melts. Part II: High pressure properties, *Geochim. Cosmochim. Acta*, *71*, 4538–4556.
- Hicks, D. G., T. R. Boehly, J. H. Eggert, J. E. Miller, P. M. Celliers, and G. W. Collins (2006), Dissociation of liquid silica at high pressures and temperatures, *Phys. Rev. Lett.*, *97*, 025502.
- Kresse, G., and J. Furthmüller (1996), Efficiency of ab-initio total energy calculations for metals and semiconductors using a plane-wave basis set, *Comput. Mater. Sci.*, *6*, 15–50.
- Kresse, G., and D. Joubert (1999), From ultrasoft pseudopotentials to the projector augmented-wave method, *Phys. Rev. B*, *59*, 1758–1775.
- Labrosse, S., J. W. Hernlund, and N. Coltice (2007), A crystallizing dense magma ocean at the base of the Earth's mantle, *Nature*, *450*(7171), 866–869.
- Mao, Z., J.-F. Lin, J. Liu, and V. B. Prakapenka (2011), Thermal equation of state of lower-mantle ferropericlase across the spin crossover, *Geophys. Res. Lett.*, *38*, L23308, doi:10.1029/2011GL049915.
- McWilliams, R. S., D. K. Spaulding, J. H. Eggert, P. M. Celliers, D. G. Hicks, R. F. Smith, G. W. Collins, and R. Jeanloz (2012), Phase transformations and metallization of magnesium oxide at high pressure and temperature, *Science*, *338*, 1330–1333.
- Mermin, N. D. (1965), Thermal properties of the inhomogeneous electron gas, *Phys. Rev.*, *137*, A1441–A1443.
- Nomura, R., H. Ozawa, S. Tateno, K. Hirose, J. Hernlund, S. Muto, H. Ishii, and N. Hiraoka (2011), Spin crossover and iron-rich silicate melt in the Earth's deep mantle, *Nature*, *473*, 199–202.
- Nomura, R., K. Hirose, K. Uesugi, Y. Ohishi, A. Tsuchiyama, A. Miyake, and Y. Ueno (2014), Low core-mantle boundary temperature inferred from the solidus of pyrolyte, *Science*, *343*, 522–525.
- Orr, R. L. (1953), High temperature heat contents of magnesium orthosilicate and ferrous orthosilicate, *J. Geophys. Res.*, *75*, 528–529.
- Perdew, J. P., K. Burke, and M. Ernzerhof (1996), Generalized gradient approximation made simple, *Phys. Rev. Lett.*, *77*, 3865–3868.
- Rivers, M. L., and I. S. E. Carmichael (1987), Ultrasonic studies of silicate melts, *J. Geophys. Res.*, *92*, 9247–9270.
- Robertson, G. S., and J. H. Woodhouse (1996), Ratio of relative S to P velocity heterogeneity in the lower mantle, *J. Geophys. Res.*, *101*, 20,041–20,052.
- Shiraishi, Y., K. Ikeda, A. Tamura, and T. Saito (1978), On the viscosity and density of the molten FeO-SiO₂ system, *Trans. Jpn. Inst. Met.*, *19*, 264–274.
- Simnad, M. T., and G. Derge (1953), Note on the nature of conduction in liquid iron oxide and iron silicates, *J. Chem. Phys.*, *21*, 933–934.

- Spaulding, D. K., R. S. McWilliams, R. Jeanloz, J. H. Eggert, P. M. Celliers, D. G. Hicks, G. W. Collins, and R. F. Smith (2012), Evidence for a phase transition in silicate melt at extreme pressure and temperature conditions, *Phys. Rev. Lett.*, *108*, 065701.
- Stackhouse, S., L. Stixrude, and B. B. Karki (2010), Determination of the high-pressure properties of fayalite from first-principles calculations, *Earth Planet. Sci. Lett.*, *289*, 449–456.
- Stixrude, L., and B. B. Karki (2005), Structure and freezing of MgSiO_3 liquid in Earth's lower mantle, *Science*, *310*, 297–299.
- Stixrude, L., and C. Lithgow-Bertelloni (2011), Thermodynamics of mantle minerals—II. Phase equilibria, *Geophys. J. Int.*, *184*, 1180–1213.
- Stixrude, L., N. de Koker, N. Sun, M. Mookherjee, and B. B. Karki (2009), Thermodynamics of silicate liquids in the deep Earth, *Earth Planet. Sci. Lett.*, *278*, 226–232.
- Thomas, C. W., Q. Liu, C. B. Agee, P. D. Asimow, and R. A. Lange (2012), Multi-technique equation of state for Fe_2SiO_4 melt and the density of Fe-bearing silicate melts from 0 to 161 GPa, *J. Geophys. Res.*, *117*, B10206, doi:10.1029/2012JB009403.
- Tsuchiya, T., R. M. Wentzcovitch, C. R. S. da Silva, and S. de Gironcoli (2006), Spin transition in magnesiowüstite in Earth's lower mantle, *Phys. Rev. Lett.*, *96*, 198,501.
- Waseda, Y., and J. M. Toguri (1977), The structure of molten binary silicate systems CaO-SiO_2 and MgO-SiO_2 , *Metall. Trans. B*, *8*, 563–568.
- Wentzcovitch, R. M., J. L. Martins, and P. B. Allen (1992), Energy versus free-energy conservation in first-principles molecular dynamics, *Phys. Rev. B*, *45*, 11,372–11,374.
- Williams, Q., and E. J. Garnero (1996), Seismic evidence for partial melt at the base of Earth's mantle, *Science*, *273*, 1528–1530.
- Williams, Q., E. Knittle, R. Reichlin, S. Martin, and R. Jeanloz (1990), Structural and electronic properties of Fe_2SiO_4 -fayalite at ultrahigh pressures: Amorphization and gap closure, *J. Geophys. Res.*, *95*, 21,549–21,563.
- Workman, R. K., and S. R. Hart (2005), Major and trace element composition of the depleted MORB mantle (DMM), *Earth Planet. Sci. Lett.*, *231*, 53–72.